Immunity
Article

Alternative Promoter Usage at the *Notch1* Locus Supports Ligand-Independent Signaling in T Cell Development and Leukemogenesis

Pablo Gómez-del Arco,[1,2,3] Mariko Kashiwagi,[3,8] Audrey F. Jackson,[3,8] Taku Naito,[3,8,9] Jiangwen Zhang,[4] Feifei Liu,[3] Barbara Kee,[5] Marc Vooijs,[6] Freddy Radtke,[7] Juan Miguel Redondo,[1] and Katia Georgopoulos[3,*]
[1]Vascular Biology and Inflammation Department, Centro Nacional de Investigaciones Cardiovasculares (CNIC), Madrid 28029, Spain
[2]Department of Molecular Biology, UAM, Madrid 28049, Spain
[3]CBRC, Mass General Hospital, Harvard Medical School, Charlestown, MA 02129, USA
[4]FAS Center for Systems Biology, Harvard University, Cambridge, MA 02138, USA
[5]Department of Pathology and Medicine, University of Chicago, Chicago, IL 60637, USA
[6]Department of Radiation Oncology (MAASTRO), GROW School for Oncology and Developmental Biology, Maastricht University Medical Center, 6200 MD, Maastricht, The Netherlands
[7]Ludwig Institute for Cancer Research, University of Lausanne, 1066 Epalinges, Switzerland
[8]These authors contributed equally to this work
[9]Present address: RIKEN Research Center for Allergy and Immunology, Kanagawa 230-0045, Japan
*Correspondence: katia.georgopoulos@cbrc2.mgh.harvard.edu
DOI 10.1016/j.immuni.2010.11.008

SUMMARY

Loss of the transcription factor Ikaros is correlated with Notch receptor activation in T cell acute lymphoblastic leukemia (T-ALL). However, the mechanism remains unknown. We identified promoters in Notch1 that drove the expression of Notch1 proteins in the absence of a ligand. Ikaros bound to both canonical and alternative Notch1 promoters and its loss increased permissive chromatin, facilitating recruitment of transcription regulators. At early stages of leukemogenesis, increased basal expression from the canonical and 5′-alternative promoters initiated a feedback loop, augmenting Notch1 signaling. Ikaros also repressed intragenic promoters for ligand-independent Notch1 proteins that are cryptic in wild-type cells, poised in preleukemic cells, and active in leukemic cells. Only ligand-independent Notch1 isoforms were required for Ikaros-mediated leukemogenesis. Notch1 alternative-promoter usage was observed during T cell development and T-ALL progression. Thus, a network of epigenetic and transcriptional regulators controls conventional and unconventional Notch signaling during normal development and leukemogenesis.

INTRODUCTION

Regulatory factors that control normal development are frequently implicated in neoplastic transformation. Ikaros, a zinc finger DNA binding protein and a key regulator of lymphopoiesis, is a prime example (Georgopoulos, 2009; Mullighan and Downing, 2008). In the hematopoietic stem cell (HSC) compartment, Ikaros is required for transcriptional priming of a lymphoid gene expression program, enabling lymphoid differentiation to the most primitive of hematopoietic progenitors (Ng et al., 2009; Yoshida et al., 2010). Normal outcome of T cell development also depends on Ikaros activity. Loss of Ikaros accelerates transition through the β-selection checkpoint, causing an aberrant accumulation of T cell receptor (TCR)$^+$ CD4$^+$CD8$^+$ "double positive" (DP) thymocytes that rapidly transit to a leukemic state (Winandy et al., 1999; Winandy et al., 1995). These phenotypes implicate Ikaros as a regulator of signaling pathways and their cellular outcome during T cell differentiation. Consistently, aberrant activation of Notch signaling occurs in Ikaros-deficient T cell leukemias, implicating Ikaros as a negative regulator of this pathway during T cell development and leukemogenesis (Chari and Winandy, 2008; Dumortier et al., 2006; Kleinmann et al., 2008; Mantha et al., 2007).

Notch signaling is another key determinant of lymphopoiesis. The Notch receptors (Notch1–Notch4) are single-pass membrane molecules that are cleaved by furin-like convertase (S1) within the Golgi secretory pathway and presented as an intramolecular heterodimer on the cell surface (Bray, 2006). Receptor engagement by a ligand presented by a neighboring cell exposes an extracellular ADAM metalloproteinase cleavage site (S2) and a γ-secretase cleavage site (S3) in the transmembrane region, releasing the Notch intracellular domain (ICN), and transmitting Notch signaling into the nucleus (De Strooper et al., 1999). ICN associates with a DNA-binding complex founded on the mammalian homolog of the recombining binding protein suppressor of hairless (RBP-Jκ, also known as CBF1) (Fortini and Artavanis-Tsakonas, 1994), which helps recruit the MAML coactivators to RBP-Jκ binding sites (Nam et al., 2006; Wilson and Kovall, 2006). These events consolidate activation of gene expression programs promoting survival and cell growth, which when deregulated lead to leukemic transformation (Palomero et al., 2006; Weng et al., 2006). Notch signaling in lymphoid progenitors (from early thymic precursor [ETP] through "double negative" 2 [DN2] stage) controls the choice between B, myeloid, and T cell fates (Radtke et al., 1999;

Sambandam et al., 2005). At the DN3 stage, Notch signaling cooperates with pre-TCR signaling to expand thymocyte numbers undergoing β-selection (Ciofani and Zúñiga-Pflücker, 2005; Garbe et al., 2006; Tan et al., 2005). Although Notch1 expression is maintained in DP thymocytes, Notch signaling is blocked at this stage. Signaling resumes in peripheral T cells, in which it controls the choice between effector cell fates (Amsen et al., 2009). More than 50% of T-ALL (T-lineage acute lymphoblastic leukemia) have Notch1-activating mutations in the heterodimerization and C-terminal PEST domains (Weng et al., 2004).

Although the connection between Ikaros loss of function and Notch activation is well established in mouse T-ALL, it remains unclear whether this interaction is direct or indirect. Loss of Ikaros may provide aberrant survival properties to differentiating thymocytes, predisposing them to further selection for activating Notch mutations and a malignant phenotype. Here, we described the use of alternative promoters within the *Notch1* locus, one of which is upstream of the canonical promoter and a second downstream within an intragenic region encoding transmembrane domains. These alternative promoters generated transcripts supporting a ligand-independent phase in Notch1 signaling and are active during T cell development and leukemogenesis. We showed that Ikaros directly regulated the epigenetic state and transcriptional output of canonical and alternative *Notch1* promoters. Deregulation of this epigenetic process during T cell development caused aberrant activation of Notch1 signaling and rapid development of T-ALL.

RESULTS

Effects of Combined Deletion of *Ikaros* and *Notch1* on T Cell Development

To evaluate the role of Ikaros in Notch-mediated transcriptional responses, we combined either of two Ikaros mutant mouse genetic models (*Ikaros* null [$Ikzf1^{-/-}$] or Ikaros dominant negative [$Ikzf1^{DN/+}$]) with a conditional inactivation model for *Notch1* that deletes a 3.7kb region encompassing the *Notch1* promoter and exon1 (Georgopoulos et al., 1994; Radtke et al., 1999; Wang et al., 1996). Thymic *Notch1* deletion with Lck Cre (Figure 1, $Notch1^{fl/fl}$ Lck Cre; $Notch1^{-/-}$), which deletes from DN3 (Lee et al., 2001), or with CD2 Cre (data not shown), which deletes from ETP (de Boer et al., 2003), gave similar results.

T cell development was evaluated in young (3–4 weeks) Notch1 and Ikaros double-deficient ($Notch1^{-/-}Ikzf1^{-/-}$) and single-deficient mice. Hallmarks of Ikaros loss of function in the thymus are a facilitation of the DN3 to DN4 transition and an increase in CD4 SP thymocytes (Winandy et al., 1999), whereas hallmarks of Notch1 loss of function are a partial block at the DN2-4 with accumulation of a DN2-3 intermediate ($CD25^{hi}$), a decrease in DP and an increase in SP thymocytes (Figure 1A) (Radtke et al., 1999). In the young $Notch1^{-/-}Ikzf1^{-/-}$ mice, a release of the previously described Notch1-loss-of-function mediated DN2-3 block (5.8% versus 14.4%), a relative increase in DP (72% $Notch1^{-/-}Ikzf1^{-/-}$ versus 58% $Notch1^{-/-}$ or 59% $Ikzf1^{-/-}$) and decrease in CD4 SP T cells (17% $Notch1^{-/-}Ikzf1^{-/-}$ versus 32% $Ikzf1^{-/-}$) compared to single deficient mice were observed (Figure 1A). *Notch1* deletion was detected in most of thymocytes in mutant mice (Figure 1B). As in the $Notch1^{-/-}$ or $Ikzf1^{-/-}$, a decrease in thymic cellularity was detected in the $Notch1^{-/-}Ikzf1^{-/-}$ mice relative to WT (Figure 1C). Notably, a reduction in CD8 SP was seen in the $Notch1^{-/-}Ikzf1^{-/-}$ thymus with almost all remaining cells displaying an immature ISP phenotype ($TCR^{-/int}/HSA^{hi}$, Figure 1D) suggesting that Notch1 and Ikaros may cooperate in the development of the CD8 SP lineage (Robey, 1999).

Notch1 Signaling in Ikaros-Mediated Leukemogenesis

Unexpectedly, from 6 weeks $Notch1^{-/-}Ikzf1^{-/-}$ mice began to develop T cell leukemia at a faster rate than $Ikzf1^{-/-}$ mice (Figure 2A). This effect of *Notch1* deletion was observed in all Ikaros mutant genetic backgrounds (Figure 2A and data not shown) and was especially prominent in mice heterozygous for the Ikaros null mutation, which usually undergo normal T cell development and develop disease at low frequency at advanced age (>6 months): the $Notch1^{-/-}Ikzf1^{+/-}$ mutants developed leukemia at high penetrance within 2–5 months. Deletion of one *Notch1* allele was sufficient to accelerate leukemogenesis, albeit at an intermediate rate compared with double deletion, indicating a gain of function provided by the mutant locus (data not shown). Unlike $Notch1^{-/-}Ikzf1^{-/-}$ or $Ikzf1^{-/-}$ mice, $Notch1^{-/-}$ mice never developed disease, indicating that the initiating event for transformation is Ikaros dependent. Accelerated tumor formation in $Ikzf1^{+/-}$ and $Ikzf1^{-/-}$ indicates the presence of an Ikaros-independent component, possibly related to deletion of a second negative regulator operating from the *Notch1* promoter.

The leukemic clones arising in the Ikaros-Notch1 compound mutants ($Notch1^{-/-}Ikzf1^{+/-}$, $Notch1^{-/-}Ikzf1^{-/-}$, and $Notch1^{-/-}Ikzf1^{DN/+}$) had a prevailing DP-transitional TCR^{int} phenotype similar to that described in $Ikzf1^{-/-}$ mice (Figure 2B and data not shown). Genomic PCR and RT-PCR analysis of these clones confirmed deletion of the *Notch1* canonical exon1 (E1c) (Figures 2C and 2D) and revealed that *Hes1* and *Il2ra* (encoding CD25) are also induced suggesting activation of Notch signaling (Figures 2B and 2D). $Notch1^{-/-}Ikzf1^{-/-}$ thymocytes in the preleukemic state (3–4 weeks, polyclonal) and leukemic state (>8 weeks, monoclonal) were further evaluated for Notch1 protein expression. $Notch1^{-/-}$ and preleukemic $Notch1^{-/-}Ikzf1^{+/-}$ thymocytes showed a similar reduction in S1-cleaved Notch1 (~120 kDa) below WT amounts (Figure 2E, lanes 2 and 4). In contrast, $Notch1^{-/-}Ikzf1^{-/-}$ or $Notch1^{-/-}Ikzf1^{DN/+}$ leukemic clones expressed large amounts of short protein isoforms (<120 kDa) not detected in WT or in preleukemic $Notch1^{-/-}Ikzf1^{+/-}$ thymocytes (Figure 2E, lanes 6, 7, and 9). One of these isoforms was recognized by an antibody to ICN (Figure 2E; Val1744, lane 9). Thus, alternative promoters supporting Notch signaling are activated at the mutant *Notch1* locus during loss-of-Ikaros-mediated leukemogenesis.

The relevance of alternative Notch1 isoforms to the leukemic phenotype of $Notch1^{-/-}Ikzf1^{+/-}$ clones was investigated. $Notch1^{-/-}Ikzf1^{+/-}$ leukemic clones lacking the canonical Notch1 isoform but expressing high amounts of alternative isoforms (Figures 2C–2E, lanes 6, 7, and 9) were monitored for their ability to grow in the presence of γ-secretase inhibitors (GSIs). Reduced proliferation in these clones indicated dependence on the alternative Notch1 isoforms that are also cleaved at S3, such as the canonical protein (Figures 2F–2H). In contrast, an independently derived $Ikzf1^{DN/+}$ clone failed to respond to GSI,

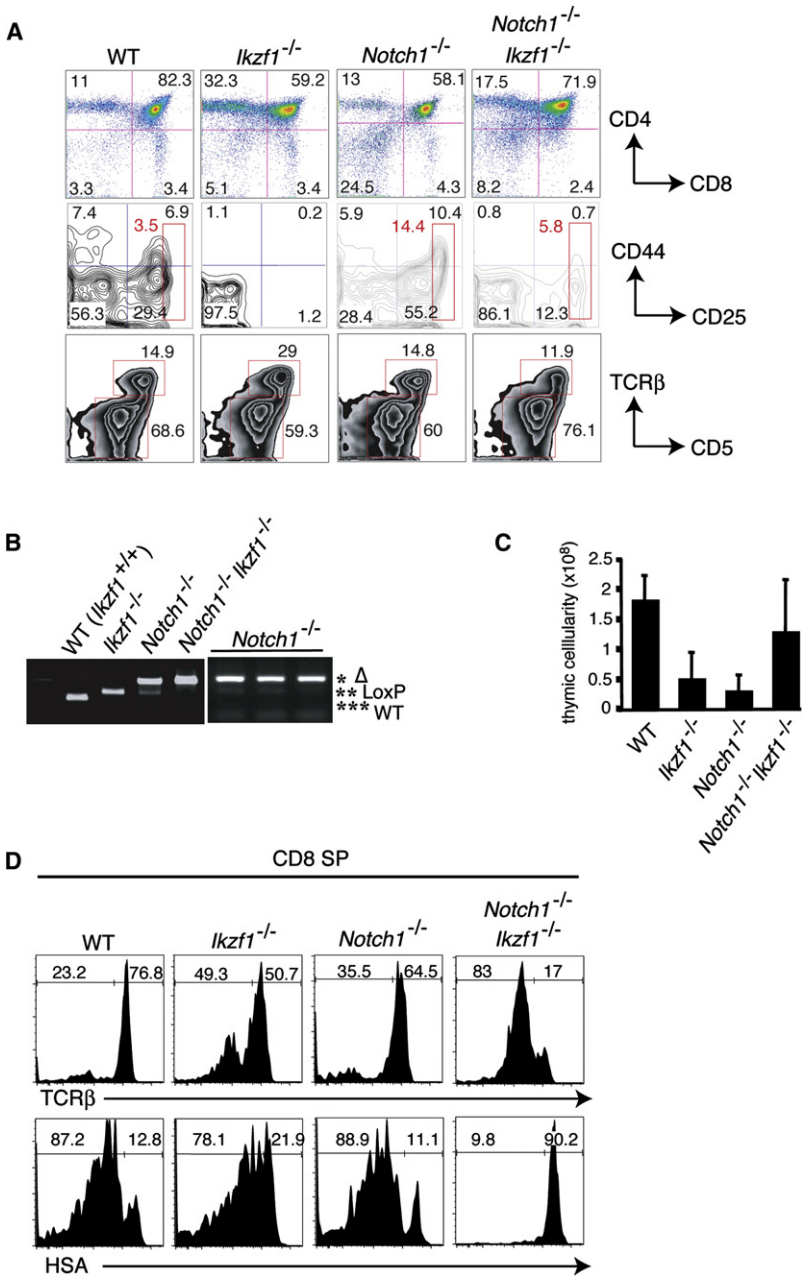

Figure 1. Combined Effects of *Notch1* and *Ikaros* Deletion on T Cell Development

(A) Thymocyte profiles of 3-week-old wild-type (WT), *Ikzf1*$^{-/-}$, *Notch1*$^{-/-}$, and *Notch1*$^{-/-}$*Ikzf1*$^{-/-}$ littermates. The upper panel shows CD4 and CD8 staining, the middle the DN1 to DN4 staining of double negative (CD4$^-$, CD8$^-$ and Thy1.2$^-$) thymocytes for CD44 and CD25. The lower panel shows expression of TCRβ and CD5 in total thymocytes. Numbers indicate the percentage of cells in each subset. Red gate shows the DN2-DN3 intermediate accumulating in the *Notch1*$^{-/-}$ thymus.

(B) Genomic PCR analysis of thymic deletion of the *Notch1* locus by LckCre.

(C) Thymic cellularities in <1.5-month-old mice (n > 5). Standard deviations (SD) are shown as error bars.

(D) CD8$^+$ SP cells shown in (A) were further evaluated for TCRβ and HSA expression.

indicating activation of an alternative transformation pathway (Figures 2F–2H).

We next combined *Ikzf1*$^{-/-}$ or *Ikzf1*$^{DN/+}$ mutants with a conditional inactivating mutation in *Rbpj*$^{fl/fl}$ CD2 Cre (*Rbpj*$^{-/-}$), the nuclear effector of Notch signaling (Tanigaki et al., 2004). A marked decrease in thymocyte cellularity and survival was observed in *Rbpj*$^{-/-}$*Ikzf1*$^{DN/+}$ or *Rbpj*$^{-/-}$*Ikzf1*$^{-/-}$ mice (3–21 weeks) (Figure 2I). Surviving *Rbpj*$^{-/-}$*Ikzf1*$^{-/-}$ thymocytes had a predominant CD4$^+$CD8$^{neg\text{-}int}$ TCR$^{int\text{-}hi}$ profile, similar to *Ikzf1*$^{-/-}$ (Figure 2J). However, unlike *Ikzf1*$^{-/-}$, *Rbpj*$^{-/-}$*Ikzf1*$^{-/-}$ thymocytes monitored from 3–32 weeks were unable to expand (Figure S1 available online). *Rbpj*$^{-/-}$*Ikzf1*$^{DN/+}$ mice did not develop detectable lymphoma even after 32 weeks, a time by which most *Ikzf1*$^{DN/+}$ mutant mice had succumbed to disease (Figure 2K and data not shown for *Ikzf1*$^{-/-}$). In the one case in which an aberrant population was observed, the expanding cells carried a wild-type *Rbpj* allele (Figure 2K and data not shown). These genetic studies indicate that Notch signaling is required for the transition of Ikaros-deficient thymocytes to a leukemic state and reveal the existence of alternative promoters in the *Notch1* locus that generate signaling-competent Notch proteins that are actively repressed by Ikaros.

Mapping of Alternative *Notch1* Transcription Start Sites

Notch1 alternative promoters and transcription start sites (TSSs) were evaluated by RNA analysis and 5′ RACE of polyA$^+$ RNA from leukemic clones arising in the *Notcht1*$^{-/-}$*Ikzf1*$^{+/-}$ and other genetic backgrounds (Figure 3). *Notch1* transcripts (~9.5 kb) containing exons 3–6 (Figure 3A and Figure S2A) were detected in WT thymocytes (~85% DP) and in *Notcht1*$^{-/-}$*Ikzf1*$^{+/-}$, *Notcht1*$^{+/-}$*Ikzf1*$^{+/-}$, and *Notcht1*$^{-/-}$*Ikzf1*$^{DN/+}$ leukemic clones (Figure 3B and Figure S2B; data not shown). 5′ RACE from exon 3 revealed splicing to exon 1a, which is 13 kb upstream of exon 1 (Figure 3A) (Tsuji et al., 2003). Transcripts (~9.5 kB) containing E1a-E3 (E1a-E3 through E34) were detected in leukemic clones but not WT DP thymocytes (Figure 3B, E1a). RT-PCR and sequencing of E1a-E3 transcripts revealed differential use of a second coding exon downstream of exon1a, previously described as exon 1b (Tsuji et al., 2003) (Figures 2D and 3A and Figure S2C). Analysis downstream of exon 24 (i.e., E25, E26, E28-31, and 34b), revealed four additional transcripts ranging in size from 3.5–5.5 kb (Figures 3B and 3C and Figures S2A and S2B). The four major short *Notch1* transcripts arise from two intragenic TSSs, one in exon 25 and a second in either intron 26 or 27 (Figure 3 and Figures S2A and S2B), and two alternative polyA$^+$ sites within exon 34 (Tsuji et al., 2003). 5′ RACE from exon 34 verified intragenic promoter usage at exon 25 and downstream intronic sites (data not shown).

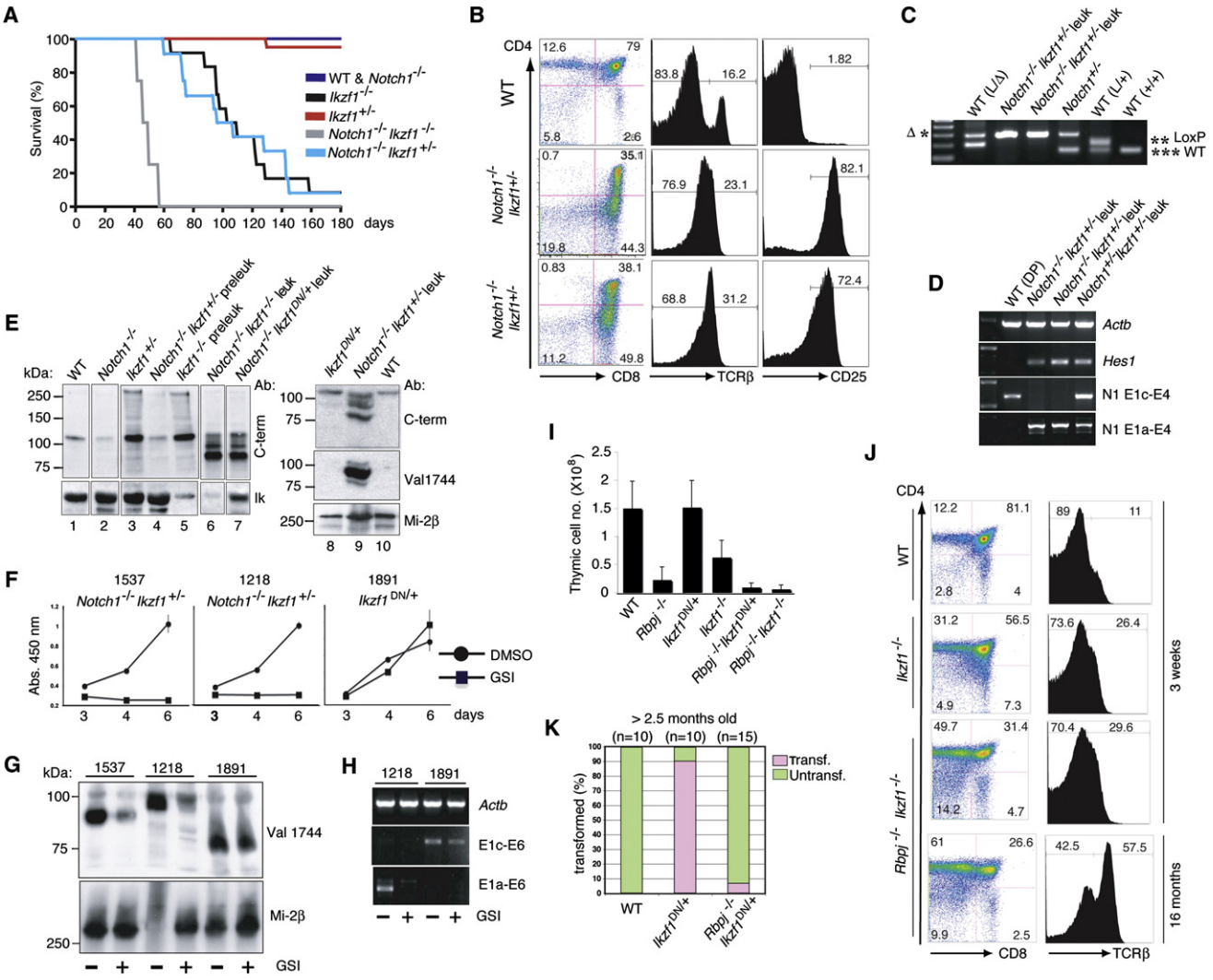

Figure 2. The Role of Notch Signaling in Loss-of-Ikaros-Mediated Leukemogenesis

(A) Kaplan-Meier survival plot for mice with different *Notch1* and *Ikzf1* mutations. All WT (n = 24) or *Notch1*$^{-/-}$ (n = 15) mice remained healthy during observation (~6 months). *Ikzf1*$^{+/-}$ mice were also generally healthy (36/38). Eleven out of the twelve *Notch1*$^{-/-}$*Ikzf1*$^{+/-}$ mice died of leukemia. Of the 12 *Ikzf1*$^{-/-}$ mice, 1 survived, 2 died of anemia, and the rest died of leukemia. All *Notch1*$^{-/-}$*Ikzf1*$^{-/-}$ (n = 5) mice died during the first 2 months of study.

(B) Thymocyte profiles of WT and two representative diseased *Notch1*$^{-/-}$*Ikzf1*$^{+/-}$ mice, as described in Figure 1A.

(C) Genomic PCR of leukemic clones deleted of the *Notch1* canonical promoter and exon 1.

(D) Semiquantitative RT-PCR of E1c from mRNAs isolated from *Notch1*$^{-/-}$*Ikzf1*$^{+/-}$ leukemic cells. Expression of *E1a*, *Hes1*, and *Actb* (control) was also detected in these cells.

(E) Immunoblot analysis of whole-thymocyte extracts at different stages of disease development with a Notch1 C-terminal (C-term) and Ikaros (Ik) antibodies. The right panel shows analysis of WT, pre-leukemic *Ikzf1*$^{DN/+}$, and leukemic *Notch1*$^{-/-}$*Ikzf1*$^{+/-}$ thymocytes with antibodies to Notch1 C terminus and also to ICN (Val1744).

(F) *Notch1*$^{-/-}$*Ikzf1*$^{+/-}$ cell lines (1537 and 1218) were treated with γ-secretase inhibitors (GSIs) and the growth was measured (See Experimental Procedures). Values of absorbance are represented as mean of triplicates from one representative experiment. The growth of an *Ikzf1*$^{DN/+}$ (1891) GSI-resistant leukemic clone is also shown. SDs are shown as error bars.

(G) Immunoblot analysis of cell-line extracts (as in E).

(H) Expression of alternative *Notch1* transcripts.

(I) Thymic cellularities of single and combined *Ikzf1* and *Rbpj* mutants at <2 months of age (n > 5). SDs are shown as error bars.

(J) Thymocyte profiles of WT, *Ikzf1*$^{-/-}$ and *Rbpj*$^{-/-}$*Ikzf1*$^{-/-}$.

(K) Frequency of leukemic transformation (pink versus green) in single and combined KO mice. All experiments were repeated at least three times, but those of (F)-(H), which were done twice.

We also analyzed production of alternative *Notch1* transcripts in leukemic clones that arise in Ikaros mutants with an intact *Notch1* promoter-exon 1 region. Alternative and canonical *Notch1* transcripts were detected in most Ikaros mutant leukemic clones (Figure 3C and Figures S2B and S2C). Activation of alternative *Notch1* TSS, either upstream of the canonical

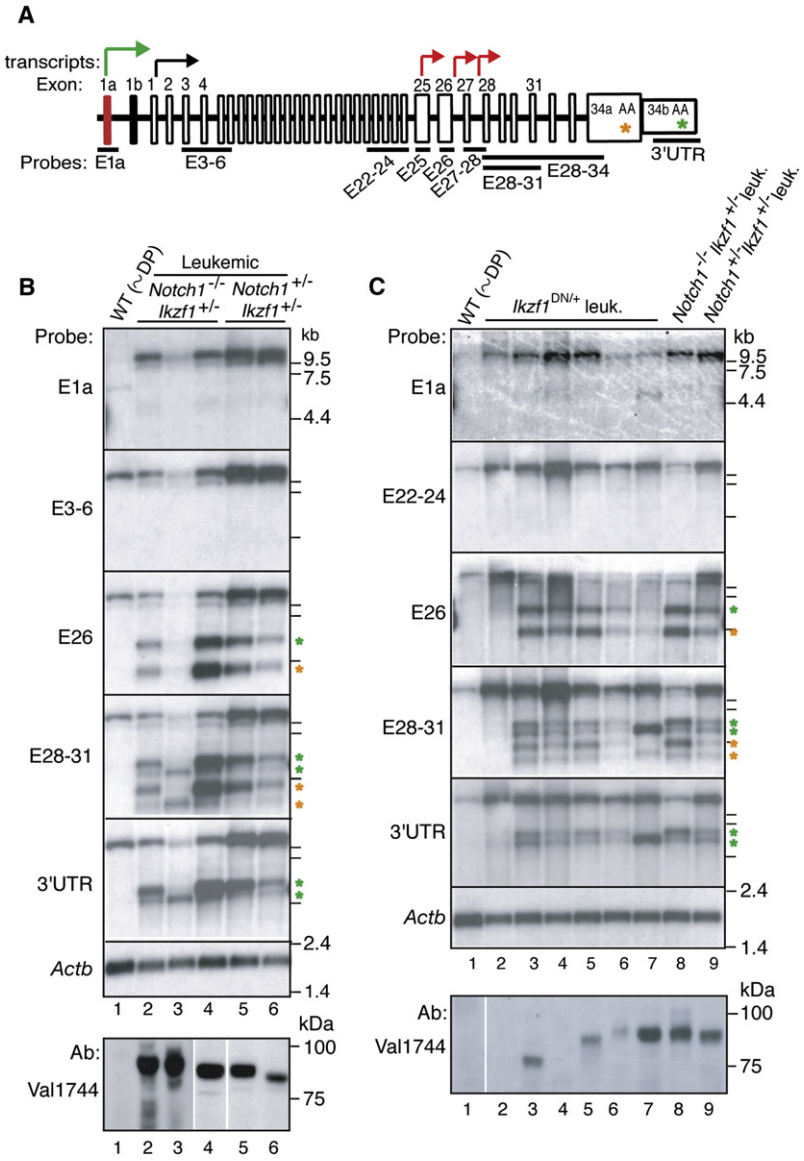

Figure 3. Mapping of Alternative TSS at the *Notch1* Locus

(A) Promoter utilization at the *Notch1* locus is shown. Green, black, and red arrows demarcate the respective 5′ alternative, canonical and intragenic TSSs described in the text. cDNA probes are shown underneath relevant regions. Open rectangles depict canonical exons, a red rectangle depicts the alternative E1a, and a black rectangle depicts the alternative E1b. Two alternative polyadenylation sites in E34 are depicted by orange or green stars. (B and C) Expression of *Notch1* transcripts and ICN in WT and leukemic cells derived from DKOs and *Ikzf1*$^{DN/+}$ mutant mice. PolyA$^+$ RNA and protein extracts were analyzed by probe hybridization (upper panels) and immunoblots (lower panel). For monitoring Notch activation, the α-Val1744 Ab was used. Transcripts with distinct polyA sites are color-coded as in (A). All experiments were repeated at least three times.

promoter or in the exon 25–28 intragenic region, correlates strongly with loss of Ikaros and activation of Notch1 ICN and is independent of deletion of the canonical *Notch1* promoter (Figures 3B and 3C and Figures S2B and S2C).

We also examined whether the effect of Ikaros on alternative promoter use was specific for *Notch1* or also manifested with other Notch family members. Although the canonical *Notch3* transcript was elevated (2- to 5-fold) in *Notch1*$^{-/-}$*Ikzf1*$^{+/-}$ and *Ikzf1*$^{DN/+}$ leukemic cells, expression of alternative transcripts from the *Notch3* locus was not detected (Figure S2D).

Utilization of *Notch1* Alternative TSSs during T Cell Development and Leukemogenesis

During T cell development, activation of Notch signaling manifests during the DN3 to DP transition, where it contributes to proliferation of immature thymocytes (Figure 4A) (von Boehmer, 2009). Notch transcriptional targets, such as *Hes1*, *Il2ra*, and *Notch1* itself, are greatly induced during this phase. We examined the activity of canonical and alternative *Notch1* promoters at these stages by testing for promoter-specific transcripts. E1c- and E1a-E3-containing *Notch1* transcripts were expressed at DN3 but progressively declined at the DN4 and DP stages, similar to *Hes1* and other Notch signaling transcriptional targets (Figures 4B and 4C). Thus, induction of canonical and 5′-alternative *Notch1* promoters is part of the Notch transcriptional response at the DN3 stage of T cell differentiation. Quantitative RT-PCR revealed higher expression of E1a-E3 containing transcripts than E1c transcripts at DN3 (Figure 4B and Figure S3A). However, at the DP stage, expression of E1c transcripts was maintained at a higher basal level (Figure 4B). RNA analysis of polyA$^+$ RNA from DN thymocytes also indicated elevated expression of E1a transcripts at this stage (Figure 4D) but did not detect the intragenic transcripts, and further analysis by RT-PCR was not possible because of interference from presplicing mRNA (data not shown).

Activation of alternative *Notch1* transcripts was next examined during leukemogenesis in Ikaros mutant thymocytes. Three major stages have been defined that demarcate the transition from a pretransformed to a transformed state and are common to thymocytes with distinct Ikaros mutations (Figure 4A and Figure S3B). Nonetheless, the rate at which different mutant cells undergo this process varies inversely with the levels of residual Ikaros and family members. The first stage is defined by Ikaros mutant thymocytes, which like WT thymocytes consist predominantly of DP with low expression of TCR (SI-DP TCR^{lo}). Thymocytes from *Ikzf1*$^{-/-}$ mice at 2–3 weeks, *Ikzf1*$^{DN/+}$ at <2 months, and *Ikzf1*$^{+/-}$ at <6 months are frequently classified as SI. The second stage is defined by an aberrant increase of cells with intermediate to high expression of TCR and a variable DP-transitional phenotype (SII- TCR^{int-hi} CD4$^+$CD8$^+$ and CD4^{lo} CD8$^+$ and/or CD4$^+$CD8^{lo}). The third stage is also categorized by a predominant TCR^{int-hi} DP-transitional

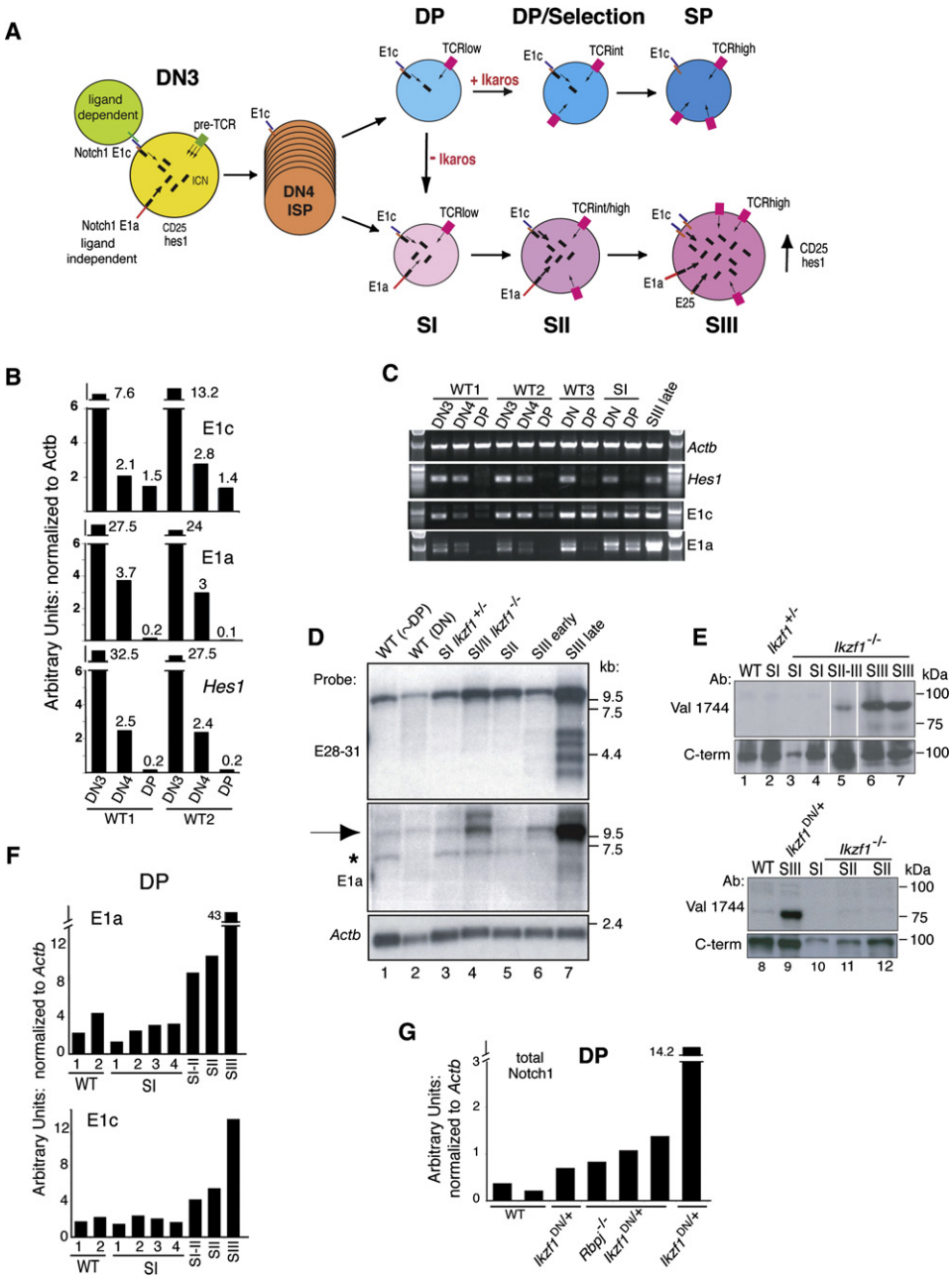

Figure 4. Expression of *Notch1* Transcripts during T Cell Development and Leukemogenesis

(A) Notch signaling during T cell development and stages of Ikaros-mediated leukemogenesis. Expression and signaling of canonical and alternative Notch1 isoforms is depicted during T cell development (DN3-SP) and leukemogenesis (stages I–III).

(B and C) Quantitative (B) and semiquantitative (C) RT-PCR with sorted DN3, DN4, and DP subsets from WT thymus and *Ikzf1* mutant clones at stages I and III. Expression of *Notch1* exon1 (E1c), exon1a (E1a) and *Hes1* transcripts was determined in (B) and (C).

(D and E) RNA (D) and protein (E) analysis of *Notch1* transcripts and ICN during Ikaros-mediated leukemogenesis (SI–SIII). The arrow in (D) marks the E1a transcript and the star marks nonspecific hybridization. Lane 2 from WT DN thymocytes was loaded with ~30% of the amount of RNA compared to lane 1 (~WT DP).

(F) Quantitative RT-PCR analysis of E1a and E1c *Notch1* transcripts in *Ikzf1* mutant DP thymocytes at stages I, II, and III.

(G) Quantitative RT-PCR analysis of total *Notch1* (exons 33–34) in $Rbpj^{-/-}Ikzf1^{DN/+}$ DP thymocytes.

population (frequently $CD4^{lo}$ $CD8^{+}$) but with a progressive increase in Notch1 signaling evident from accumulation of ICN and increased levels of its transcriptional targets (SIII early-late TCR^{int-hi} ICN^{lo-hi}, $CD25^{lo-hi}$, $Hes1^{neg-hi}$) (Figures 4A, 4C, and 4E and Figure S3B). Notably, clonality among the expanding TCR^{int-hi} mutant thymocytes was detected both before and upon Notch activation (Figure S3C, SI–SIII). Thus clonal expansions can be initiated in the absence of Notch signaling; however, the aggressive leukemic clones predominant at late stages are mostly Notch dependent.

Quantitative RT-PCR and RNA analysis of Ikaros mutant thymocytes detected modest elevation of the 5′ canonical and alternative *Notch1* transcripts by SII (Figures 4D–4F; E1c and E1a; 2- to 3-fold). By SIII, marked by ICN accumulation, E1a and E1c transcripts were further induced (Figures 4D–4F, >10-fold). The increase in basal transcription from *Notch1* promoters was also seen in $Rbpj^{-/-}Ikzf1^{DN/+}$ thymocytes, indicating that this is a direct effect of Ikaros and not caused by Notch signaling manifested in a minority of the population (Figure 4G). Activation of the *Notch1* intragenic promoters lagged behind the E1a and E1c promoters, given that their corresponding transcripts were first detected at low level in early SIII (Figure 4D, lane 6). These, together with the full-length (i.e., E1c- and E1a-) transcripts, were further induced upon ICN accumulation in late SIII leukemic clones (Figure 4D, lane 7 and 4E, lanes 5–7 and 9).

Thus, the 5′ alternative and canonical *Notch1* promoters are part of a regulatory mechanism operative during both development and leukemogenesis. The increase in basal transcription from the 5′ promoters in the preleukemic state coincides with reduced Ikaros activity. A further robust induction of both the 5′ and the intragenic *Notch1* alternative promoters is detected at later leukemogenesis stages and coincides with ICN accumulation.

Function of Proteins Encoded by Alternative *Notch1* Transcripts

The structure and activity of proteins generated by the alternative *Notch1* transcripts was assessed in cell culture. The proteins encoded by the canonical *Notch1* transcript (E1c: exon 1–34), the 5′ alternative transcript (E1a-E3: exon 1a–3–34), and the longest intragenic transcript (E25: exon 25–34) were expressed from a construct in which the C terminus PEST domain was either replaced by a 6-Myc tag (Figures 5A–5C; E1a-E3 6MT, and E1c 6MT) or left intact (Figure 5D, E25 and E1c; and data not shown for E1a-E3) (Kopan et al., 1996; Mizutani et al., 2001). Notch1 ICN with an intact PEST domain served as a positive control (Figure S4, ICN) (Aster et al., 2000). Similar results were obtained with these vectors in HEK293T (Figure 5) and U2OS cells (data not shown). The low amount of ICN detected upon expression of the canonical *Notch1* transcript in HEK293T indicated low amounts of either ligand-receptor engagement or constitutive Noch1 S3 cleavage in these cells.

The E1a-E3 *Notch1* transcript supported higher amounts of ICN production, nuclear localization, and activation of the RBP-Jκ reporter than the canonical transcript, although both expressed recombinant Notch1 proteins at similar levels (Figures 5B and 5C and Figure S4). GSI treatment reduced the amounts of proteins generated by the E1a-E3 transcript, indicating dependence of Notch signaling on processing (Figure 5B). In addition to Notch1 proprotein (yellow star), the E1a-E3 transcript produced a cleaved isoform that migrated more quickly than the constitutively furin-cleaved protein (S1, green arrow) produced by the E1c transcript (Figures 5A and 5B and Figure S4). This protein was specifically recognized by an antibody to the S2-cleaved Notch1 (S2-Val1711, yellow arrow), normally induced upon ligand binding to the receptor (van Tetering et al., 2009). The apparently constitutive processing of the E1a-E3 protein by S2 and S3 (Val1744, purple arrow) was verified by immunoblotting and immunofluorescence (Figures 5B and 5C). GSI increased the S2 product and decreased the S3 product, further supporting constitutive S2 cleavage of this isoform (Figure 5B). Consistent with its S2-S3 processing, the E1a-E3 isoform (but not E1c), was frequently detected in nuclei (Figure 5C).

The E25 transcript generated a range of short proteins that stimulate RBP-Jκ reporter activity through ICN production (Figure 5D). GSI reduced reporter activation by these isoforms, indicating that their activity is also dependent on S3 cleavage. Nonetheless, unlike E1a-E3 there was no accumulation of an S2 product, indicating translation downstream of this site (Figure 5D, and data not shown). The six putative translation initiation methionines in the E25 transcript were next evaluated by mutagenesis (Figures 5A and 5E and Figure S5). Methionine to alanine substitution at position 1727 (E25: M1727A) abolished the major isoform (Figures 5E, red asterisk and Figure S5). Interestingly, mutations of downstream methionines (M1796A, M1845A, and M1848A; blue stars) increased translation from M1727 and reporter activity, indicating that competition between alternative translation sites may modulate Notch signaling driven by the intragenic transcripts (Figure 5E, Figure S5, and data not shown).

The 5′ and intragenic *Notch1* promoters thus generate stronger transcriptional activators than the canonical promoter. In both cases this is due to the production of proteins whose cleavage by ADAMs and/or γ-secretase is either accelerated or occurs constitutively when ligand is limiting.

The Role of Ikaros in Dictating Chromatin Accessibility at the *Notch1* Locus

Transcriptional output is partly determined by local enhancer and promoter chromatin regions that control access to the basal transcriptional machinery and regulators. We examined the histone modifications H3K4me3, H3K27me3, H3K36me3, and H3K9/14ac at the *Notch1* locus in WT and Ikaros mutant thymocytes at stage II (SII-DP TCR^{int-hi}) prior to activation of Notch signaling. Combinations of these modifications provide a measure of transcriptionally active (H3K4me3, K9/K14ac, and K36me3), poised (H3K4me3 and K9/K14ac; H3K4me3, K9/K14ac, and K27me3; H3K4me3 and K27me3) and repressed (H3K27me3) chromatin (Campos and Reinberg, 2009; Mendenhall and Bernstein, 2008; Schones and Zhao, 2008). We used chromatin immunoprecipitation coupled to high-throughput sequencing (ChIP-Seq) to compare the chromatin status of genes in total thymocytes mostly at the DP stage (~85%) with that of genes expressed in DN, DP, or SP populations. Enrichment in H3K36me3, a chromatin marker of long-range transcription elongation, was seen only in genes expressed in DP cells (Figure S6).

Islands of H3K4me3 and H3K9/K14Ac are found primarily in promoter regions and are in part generated by recruitment of the transcription initiation complex (Guenther et al., 2007). In WT DP, a major H3K4me3/H3K9/K14ac island was detected at the canonical *Notch1* promoter (Figure 6A). A minor island was detected ~13 kb upstream, spanning E1a and further validating this region as an alternative 5′ promoter (Figure 6A). No H3K4me3 or H3K9/K14ac islands were detected in the *Notch1* intragenic region in WT DP thymocytes. This indicates that the intragenic promoters are neither active nor poised, consistent with Notch1 transcript analysis at the DN and DP stages (Figures 4B–4D). H3K36me3 was detected downstream of the canonical

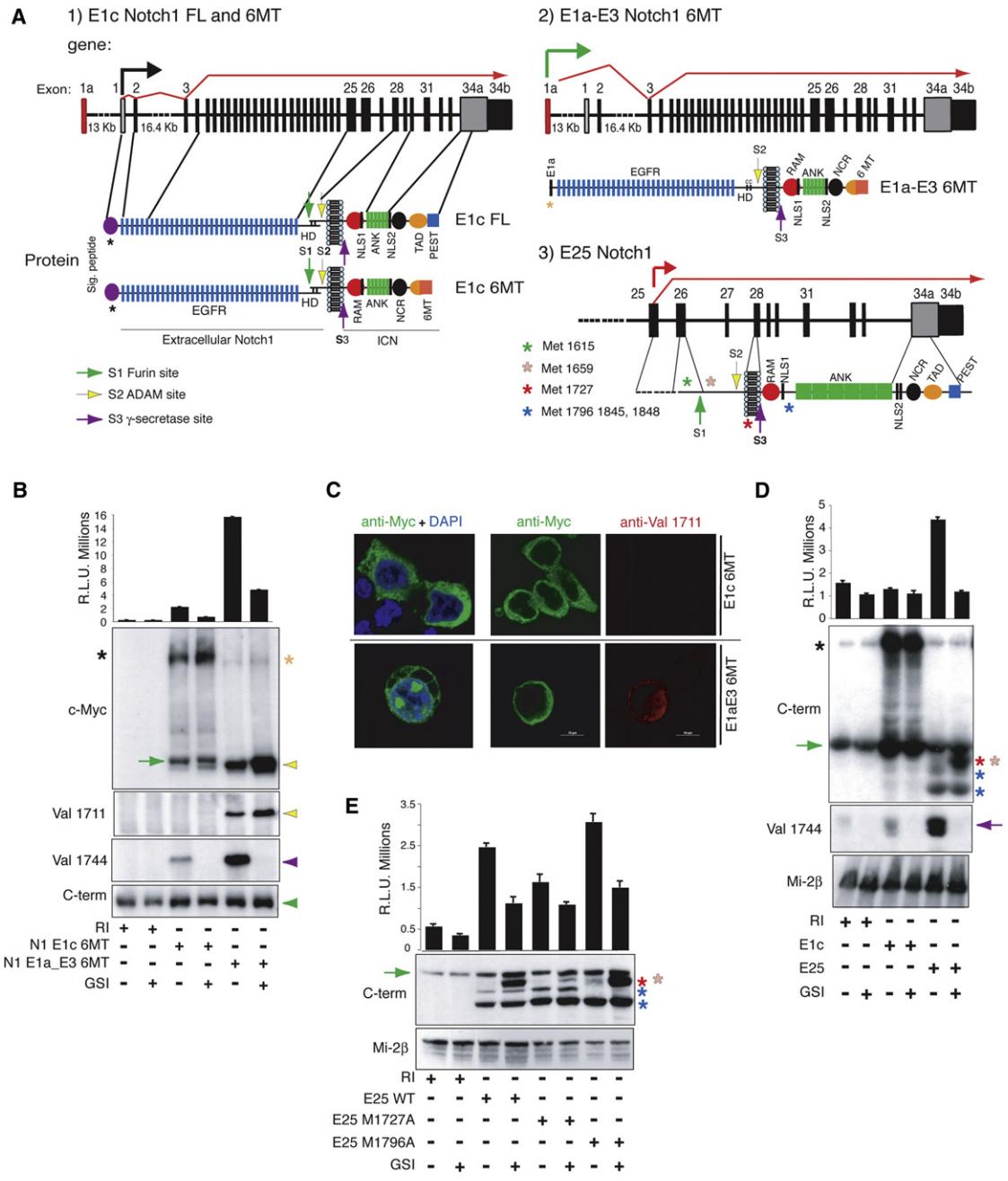

Figure 5. Ligand-Independent Signaling Provided by Alternative Notch1 Isoforms

(A) Exon and protein domain composition of the canonical (E1c) and alternative *Notch1* transcripts (E1a-E3 and E25, see also Figure S5). Notch1-translated isoforms are depicted with asterisks: black, 300 kDa canonical (E1c FL and 6MT); and orange, exon 1a (E1a-E3 6MT) proproteins; green, M1615; pink, M1659; red, M1727; and blue, M1796, M1845, and M1848 and by processing with arrows: green, S1 site; yellow, S2 site; and purple, S3 site. The construct substituted the PEST domain by a 6 MYC-tag is depicted 6MT and with the intact C terminus FL.

(B and C) The activity and cellular localization of the E1a-E3 transcript (E1a-E3 6MT) was compared to that of the canonical (E1c 6MT). Expression vectors were cotransfected with the RBP-Jκ pGALuc reporter into HEK293 cells and assayed for relative luciferase units (RLUs) (as light units measure in 10 s.) and recombinant protein production by immunoblotting and immunofluorescence with antibodies to the c-Myc, the S2 (Val1711), and S3 (Val1744) epitopes as well as to a C-terminal domain. Notch1 proteins are demarcated by asterisks as in (A). A representative experiment out of three is shown.

(D) Notch1 protein production and activity was also assessed in the presence (+) or absence (–) of GSI. The proteins generated by the alternative E25 transcript were tested for activity relative to the E1c FL. Reporter activity and protein analysis were performed as in (B).

(E) Mutational analysis mapped a major as well as minor translation sites within the E25 transcript. Expression studies were performed as in (B) and (D). Asterisks indicate distinct translation products as in (A). All experiments were repeated at least three times. SDs are shown as error bars.

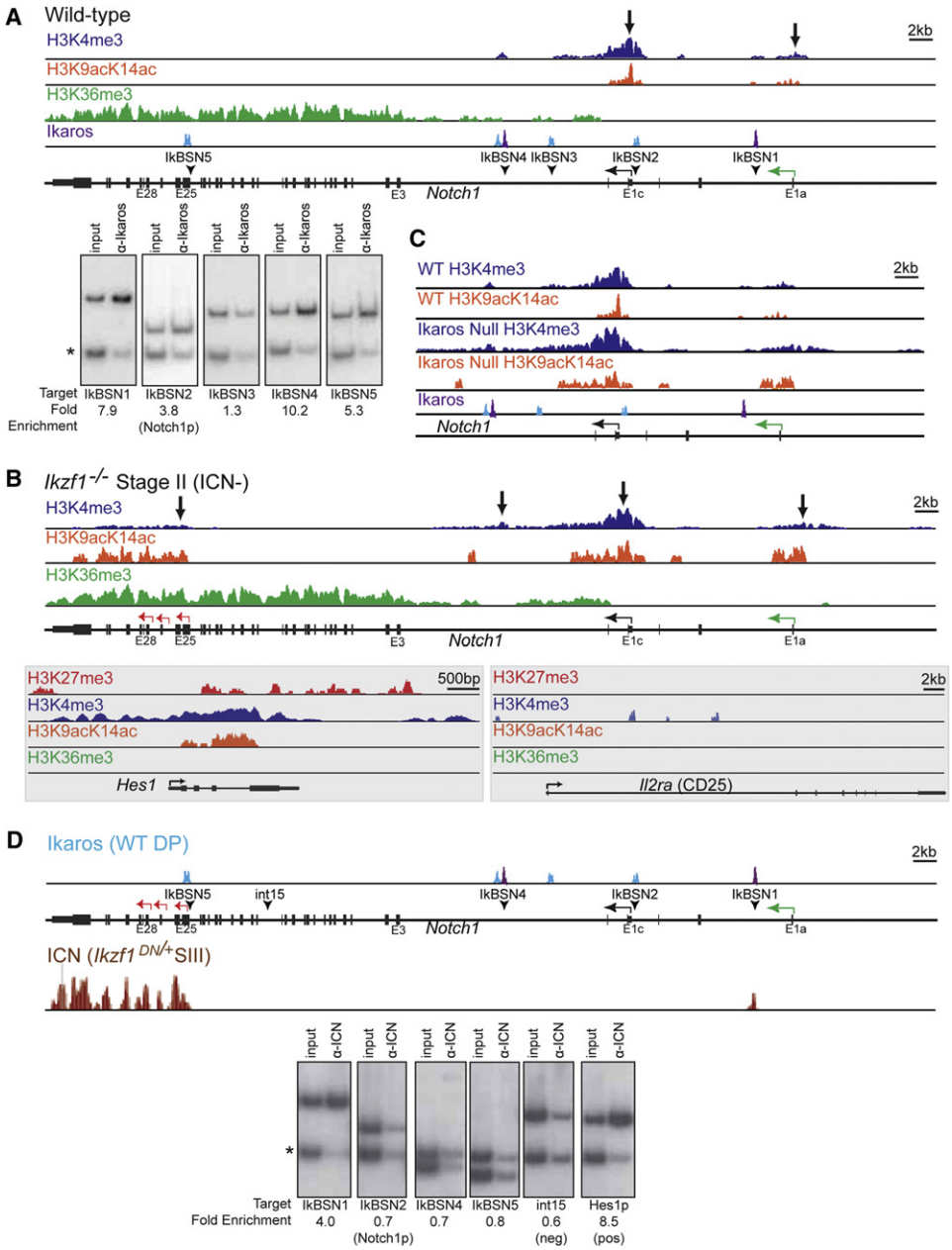

Figure 6. Loss of Ikaros Binding to *Notch1* Locus Affects the *Notch1* Chromatin Environment

Peaks are shown for ChIP-Seq performed with anti-H3K27me3 (red), anti-H3K4me3 (blue), anti-H3K9/14ac (orange), anti-H3K36me3 (green), anti-Ikaros (purple and light blue), and anti-ICN (dark red). The *Notch1* canonical promoter (black arrow), 5′ alternative promoter (green arrow), and intragenic alternative promoters (red arrows) are identified.

(A) Histone modification status and Ikaros binding at *Notch1* locus in WT DP thymocytes. Islands of H3K4me3 and H3K9/14ac (black vertical arrows) decorated the transcriptionally active E1c promoter and poised E1a promoter. *Notch1* expression in DP thymocytes was confirmed by the H3K36me3 elongation mark. High confidence (purple, p value 10^{-5}), and lower confidence (light blue, p value 10^{-3}) Ikaros-binding sites were identified at the promoters and at intragenic locations and validated by ChIP-PCR. An asterisk marks the internal control in duplex ChIP-PCR.

(B) Histone modification status at the *Notch1* locus in Ikaros null SII thymocytes that have not activated Notch signaling.

(C) A direct comparison (equal tag numbers) of histone modifications at the E1c and E1a promoters. IkBS relative to methylation and acetylation islands are also indicated.

(D) Notch1 ICN binding at *Notch1* at late stage III of leukemogenesis. Binding of ICN was examined by ChIP-Seq and candidate ChIP at four Ikaros binding sites, at intron 15 (negative control) and at the *Hes1* promoter (positive control). These experiments were repeated twice with similar results.

TSS, in line with its reported accumulation after transition from short-term to long-term elongation (Joshi and Struhl, 2005). H3K27me3, which marks a restrictive chromatin state, was not detected at the *Notch1* locus (data not shown).

ChIP-Seq for Ikaros identified two high-confidence Ikaros-binding sites (IkBS) (p value 10^5) ~10 kb upstream and downstream of the canonical TSS (Figure 6A; IkBSN1 and IkBSN4, purple). The upstream Ikaros site is within 3 kb of the E1a promoter. Notably, both sites are in minor H3K4me3 islands. Four lower-confidence IkBS (p value 10^{-3}) were also found: one at the E1c promoter, two at the intron 2 and one at the E25 promoter (Figure 6A, IkBSN2, IkBSN3, IKBSN4 and IkBSN5, blue). ChIP-PCR validated the high-confidence Ikaros sites as well as two of the lower confidence sites (IkBSN2 and IkBSN5).

We next analyzed the chromatin status of the *Notch1* locus in *Ikzf1*$^{-/-}$ preleukemic thymocytes before activation of Notch signaling (Figure 6B, stage II: ICN$^-$). Cell staging was validated by testing for H3 modifications at Notch1 targets such as *Hes1* and *Il2rα*. Both genes lacked the elongation marker H3K36me3 (Figure 6B). Furthermore, *Hes1* retained H3K27me3 and H3K4me3 throughout the locus, consistent with a bivalent and repressed state in DP cells. In contrast, the *Notch1* locus displayed an increase in H3K4me3 and H3K9/K14ac islands spanning the 5′ canonical (E1c) and the alternative (E1a) promoters (Figures 6B and 6C). Increased intensity and range of H3K36me3 was also seen, consistent with the increase in basal transcription from the E1c and E1a promoters in SII mutant thymocytes. In addition to the increase in H3K4me3 and H3K9/K14ac at the 5′end of *Notch1*, a group of de novo H3K4me3 and H3K9/K14ac islands was detected at the intragenic region, starting at E25 and extending into the 3′ end (Figure 6B). These H3K4me3 and H3K9/K14ac islands encompass the intragenic promoter region that is activated upon ICN accumulation at SIII of leukemogenesis. These data highlight that the genomically intact *Notch1* locus acquires a more permissive chromatin configuration at its canonical and alternative promoters before their robust induction by ICN.

Given reports that Ikaros and ICN work through the same DNA sequences (Beverly and Capobianco, 2003), we examined the distribution of ICN at the IkBS of *Notch1* in SIII leukemic cells by ChIP-PCR (Figure 6D). Strong ICN enrichment was detected at IkBSN1 but not at downstream sites (Figure 6D). As previously reported, ICN was highly enriched at the *Hes1* promoter. Binding of ICN at IkBSN1 was confirmed by ChIP-Seq, which also revealed a striking distribution within the intragenic methylation and acetylation islands starting downstream of IkBSN5 in E25 (Figure 6D).

These epigenetic studies provide insight into the transcriptional regulation of *Notch1* promoters in WT, preleukemic, and leukemic thymocytes and establish a direct role for Ikaros in restricting chromatin accessibility at these regulatory sites.

Further Delineation of *Notch1* Regulatory Regions Reveals E2A as a Contributing Factor

The *Notch1* promoter regions and Ikaros binding sites were next evaluated in silico for *cis*-element composition (Figure 7). A large CpG island surrounded E1c, as is typical of 50%–70% of mammalian promoters (Sandelin et al., 2007). Coincident with the CpG island was an array of GC boxes, which can bind the transcriptional activator Sp1. The 5′ alternative promoter E1a did not have these elements, suggesting it is normally weak and may need recruitment of additional factors for activation (Figure 7A). Strong cross-species conservation was detected for the E1a promoter region, supporting its functional importance (data not shown). A set of classic promoter elements is found in the intragenic region, particularly upstream of E28. This intragenic TSS contains a CpG island and TATA, CCAAT, and GC boxes at appropriate upstream distances, indicating a capacity for strong transcription when this region is accessible (Figure 7A, lower panel). This is consistent with the evidence that binding of Ikaros and possibly other factors is necessary to restrict access to this site.

Sequence analysis identified many potential transcription factor binding sites, including several clusters of E2A motifs within or near IkBS sites (Figure 7A). One site is directly upstream of the canonical promoter close to IkBSN2, two are just downstream of the canonical CpG island and one is within IkBSN4, the IkBS 10 kb downstream from the promoter (not shown). Several E2A sites are located directly upstream of the TSS in E1a. In the region of the intragenic promoters, a cluster of E2A sites extends downstream of IkBSN5 in E25 into E26, another cluster is found in intron 26, and another is found in intron 29. Given the abundance of E2A sites and their proximity to *Notch1* regulatory regions, we examined *Notch1* promoter use in E2A deficient (*Tcf3*$^{-/-}$) primary leukemic clones and cell lines with active Notch signaling (Figure 7B and Figure S7) (Reschly et al., 2006). Alternative *Notch1* transcripts predominated in these clones, indicating that Ikaros and E2A participate in a common mechanism of leukemic transformation. E2A binding to multiple regulatory elements in the *Notch1* locus, especially sites at the deleted canonical *Notch1* promoter region, provide a plausible explanation of the acceleration of leukemogenesis upon *Notch1* promoter deletion in Ikaros mutant thymocytes.

DISCUSSION

Here, we showed that the *Notch1* locus is regulated by a combination of transcriptional promoters and enhancers supporting a feed-forward loop that probably augments Notch signaling at appropriate stages of T cell differentiation and leukemic transformation. Ikaros is one of the key regulators in this process working at the epigenetic level to limit recruitment of transcription-related factors.

The presence of alternative promoters at the *Notch1* locus was first revealed by studies in leukemic cells from mice with combined mutations in *Ikzf1* and the *Notch1* canonical promoter. Although activity of the alternative *Notch1* promoters was augmented in the *Notch1*$^{-/-}$*Ikzf1*$^{+/-}$ leukemic cells, it was also elevated in other leukemia models in which the canonical *Notch1* promoter was intact. Nonetheless, combined deletion of the *Notch1* canonical promoter and *Ikzf1* accelerated this process, indicating participation of additional negative regulatory factors acting through the deleted region. A likely candidate is E2A because it binds at the canonical *Notch1* promoter (Yashiro-Ohtani et al., 2009) and has similar effects as Ikaros on Notch1 transcriptional regulation and leukemogenesis. These studies also show that in T cells, the *Notch1* exon1 deletion is not a null allele, particularly under conditions in which active Ikaros repression is

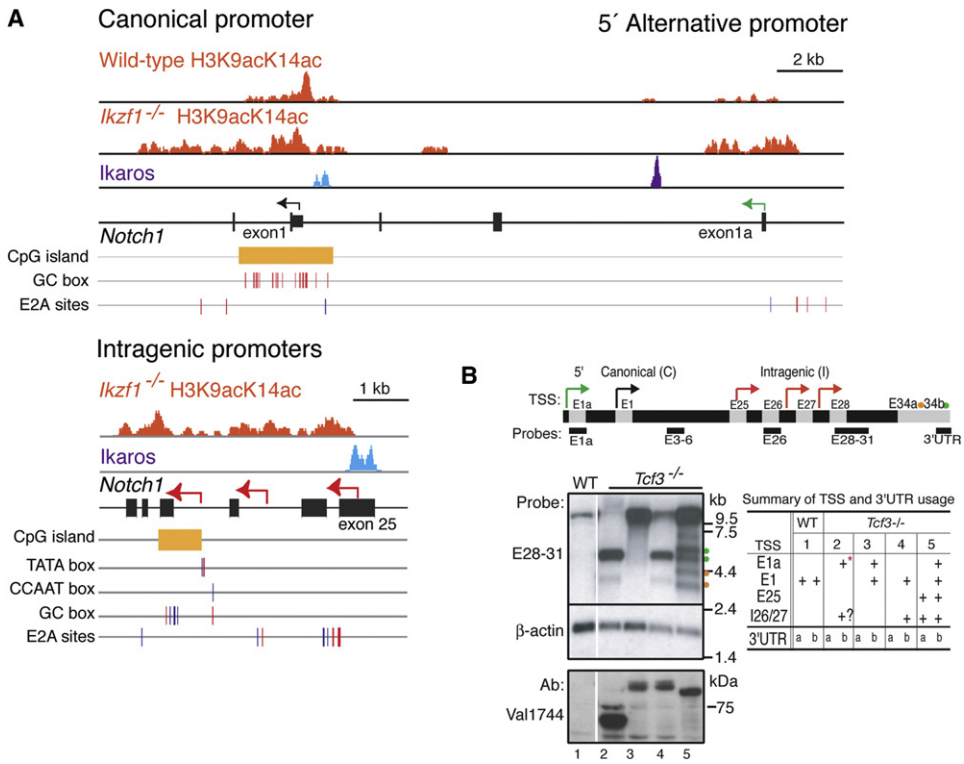

Figure 7. Ikaros and E2A Coregulate Canonical and Alternative *Notch1* Promoters

(A) Sequence analysis of the canonical and alternative promoter regions identified four promoter elements—CpG islands and TATA, CCAAT, and GC boxes—and binding sites for E2A within or near regions of Ikaros binding. IkBSs sites are purple or light blue. Promoter elements and putative E2A sites are represented in blue (+ strand) or red (− strand).

(B) *Notch1* alternative transcripts and ICN protein were detected in *Tcf3*$^{-/-}$ leukemic cells. Exons in the vicinity of transcription start sites and 3′ UTR are indicated with gray boxes. The table summarizes the usage of each TSS and 3′ UTRs.

relaxed. Although it is possible that this allele is an effective null in other contexts, it will be important to assess whether deletion of negative regulatory elements and de-repression of these ligand-independent isoforms occurs in other cell types.

In addition to the canonical promoter, two alternative *Notch1* promoter regions were mapped at the 5′ and at an intragenic location. Transcriptional analysis of the *Notch1* locus during normal T cell development indicated that at the DN3 stage, both the 5′ alternative and canonical promoters were active, whereas at the DP stage, only the canonical promoter retained activity. Epigenetic studies in DP thymocytes confirmed the presence of permissive chromatin at the active promoter but also indicated that the inactive 5′ alternative promoter was in a permissive chromatin configuration possibly poised for future transcriptional induction upon activation of Notch signaling. In contrast to the 5′ promoters, the intragenic promoter region was transcriptionally repressed through the DN3-to-DP transition, was not marked for transcriptional activation at the chromatin level, and displayed extensive Ikaros binding.

During loss of Ikaros-mediated leukemogenesis, all three sets of *Notch1* promoters acquired more permissive chromatin prior to activation of Notch signaling. Increase in permissive chromatin was detected at the 5′ alternative and canonical promoters and most notably at the intragenic promoters in preleukemic thymocytes on an intact *Notch1* locus. The increase in chromatin accessibility at the 5′ *Notch1* promoters correlated with an increase in basal transcription detected at the preleukemic state that preceded the strong transcriptional induction detected upon ICN accumulation at the leukemic state. Importantly, inhibition of Notch signaling, through γ-secretase inhibition or by *Rbpj* inactivation, interfered with the robust transcriptional induction at both the canonical and alternative promoters in leukemic cells but did not alter the increase in basal transcription observed in preleukemic thymocytes.

Both alternative promoters were responsible for the production of proteins that signal in limiting ligand. The full-length Notch1 protein generated by the E1a promoter lacks the signal peptide present in the canonical unprocessed form and appears to be processed differently. Notably, it is constitutively cleaved by ADAM metalloproteinases (S2) and γ-secretase (S3) in limiting ligand conditions. Thus, alternative 5′ promoter and exon usage may dictate an alternative route of cell trafficking and receptor processing that enhances Notch signaling that is pending further investigation. A range of short Notch1 protein isoforms was produced by the intragenic promoter region. A major isoform was translated from a site downstream of the S2 or ADAM site that lacked the ligand binding and NRR domains and was a potent activator of the Notch transcriptional response.

Given these data we propose the presence of a feedback loop in Notch signaling supported by a network of epigenetic and

transcriptional regulators and Notch receptors with differential ligand dependence for activity. Local chromatin at the *Notch1* locus controls access to the basal transcription machinery and to enhancer proteins that regulate this process. The presence of Ikaros at binding sites located in proximity to all three *Notch1* promoters is responsible for restricting chromatin. Ikaros association with negative chromatin-remodeling factors such as Mi-2β and HDACs may restrict access or activity of positive chromatin regulators such as MLL and HATs also recruited to these sites (Kim et al., 1999; Sridharan and Smale, 2007). Loss of Ikaros relieves chromatin restriction, increasing access to the basal transcription machinery at both ligand-dependent and -independent *Notch1* promoters. This precipitates a forbidden increase in ICN, which even if present at low amounts is more effectively recruited to its target sites that are more accessible because of Ikaros removal. ICN is a potent transcriptional enhancer that can function from at least two regions in the *Notch1* locus. One is at the promoter-distal IkBSN1, and the second is at an extended region downstream of the IkBSN5 in E25. Importantly, this ICN-binding region shows extensive overlap with the de novo intragenic islands of permissive chromatin arising in Ikaros mutant preleukemic cells. Interactions of ICN with HATs (Wallberg et al., 2002) at its target sites may further impact transcription initiation. Transcription of the *Notch1* locus is probably affected by a number of regulatory factors. In addition to Ikaros and E2A, our preliminary studies indicate a similar aberrant activation of alternative *Notch1* promoters in abnormally expanding DP in an activated Akt2 transgenic model (data not shown) (Malstrom et al., 2001). Thus, both nuclear and signaling factors implicated in leukemogenesis may participate in the regulation of this feed-forward loop in Notch signaling.

Stage-specific activation of the *Notch1* promoters may be one key for modulating levels of Notch signaling during development and leukemogenesis. The induction of promoters expressing isoforms with differential ligand requirement may support a feed-forward mechanism that augments Notch signaling required for expansion of immature thymocytes. At the DN3 stage, this may be jump-started by the ligand-dependent canonical Notch1 E1c isoform and propagated by the more active E1a isoform. Subsequently at the DP stage, the E1a promoter is repressed and only the canonical promoter remains modestly active. Together with limited ligand availability, this may restrict Notch signaling to levels supporting cell survival and not proliferation at this stage of differentiation (Laky and Fowlkes, 2008). In the *Notch1*-deficient cells, deletion of the canonical promoter and lack of expression of the ligand-dependent Notch1 isoform prevented activation of the 5′ alternative promoter under conditions of restrictive chromatin. However, upon loss of Ikaros (and possibly E2A), aberrant increase in chromatin accessibility augments basal transcription at the alternative *Notch1* promoters, marking transition to a preleukemic state. This allows a progressive increase in ICN accumulation that eventually causes robust induction of both ligand-dependent and -independent *Notch1* promoters, thus sealing the transition to the leukemic state. Aberrant activation of the *Notch1* promoters collaborates with Notch1 mutations that target the PEST domain in the mouse genetic systems studied here to exacerbate the leukemia phenotype. It will be important to determine whether such a mechanism is also manifested in human leukemia in which a predominance of mutations in the heterodimerization and PEST domains has been described. Strong cross-species conservation of both the canonical and alternative promoters gives support. Targeting the transcriptional regulation of *Notch1* may open new avenues for leukemia treatment. Small molecules targeting enzymes that control chromatin accessibility in combination with γ-secretase inhibitors may provide better treatment protocols for curing T-ALL.

EXPERIMENTAL PROCEDURES

Mice

Ikzf1$^{-/-}$, *Ikzf1*$^{DN/+}$ (Georgopoulos et al., 1994), *Notch1*$^{fl/fl}$ (Radtke et al., 1999), and *Rbpj*$^{fl/fl}$ mice (Radtke et al., 1999; Tanigaki et al., 2002; Wang et al., 1996) were bred and housed under pathogen-free conditions. The *Notch1* and *RBP-Jκ* deficient strains were maintained as intercrosses to either lck-Cre or hCD2-Cre (de Boer et al., 2003; Lee et al., 2001).

Cell Culture and Proliferation Assays

Notch1$^{-/-}$*Ikzf1*$^{+/-}$ and other mutant cell lines established from primary thymic lymphomas were maintained in RPMI media as described in the Supplemental Information.

Flow Cytometry

Phenotypic analysis of thymocytes and splenocytes was performed by flow cytometry with FACSCanto (BD) or MoFlo (Cytomation). Data were analyzed with the FloJo software (Tristar). The antibodies used in this study were CD4-PE-Cy5.5 (or CD4-PE-Cy7), CD8α-APC-Cy7, TCRβ-APC, CD5-PE, CD25-PE (or CD25-APC-Cy7), HSA-PE, CD69PE, Thy1.2-PE, CD62L-APC, and CD44-APC as previously described (Williams et al., 2004).

D-J Rearrangement and *Notch1* and *Rbpj* Deletion Analyses

TCRβ D-J rearrangement as well as deletion at the *Notch1* and *Rbpj* loci were examined by genomic PCR as previously described (Winandy et al., 1995).

RT-PCR, Rapid Amplification of 5′ End of cDNAs and RNA Analysis

The cDNA was synthesized from RNA with SuperScriptII RTase (Invitrogen). For qRT-PCR, transcripts were amplified with HotStart-IT SYBER Green qPCR Master mix (USB) on the ABI sequence detection system (Applied Biosystems). All qRT-PCR reactions were performed in triplicate.

For rapid amplification of 5′ end of cDNAs (RACE), the first strand cDNA was synthesized with 1 μg polyA$^+$-selected RNA using the SMARTER RACE cDNA Amplification kit (CLONTEC) according to the manufacturer's instructions. For Northern analysis, standard protocols were used.

Immunoblotting and Immunofluorescence Studies

The antibodies used for these studies were anti-Notch1, anti-c-Myc (9E10) (Santa Cruz), anti-cleaved Notch1 (S2, Val1711) (van Tetering et al., 2009), anti-Cleaved Notch1 (S3, Val1744) (Cell Signaling Technology, anti-PSF (B92) (Sigma), or anti-Mi-2β (Williams et al., 2004). For immunofluorescence (IF), cells were grown and transfected with the indicated plasmids on chamber slides. Forty-eight hours after transfection, cells were fixed with 4% PFA and processed for IF as previously described (Gómez-del Arco et al., 2005). Images were taken with a Nikon A1R confocal microscope.

Chromatin Immunoprecipitation and ChIP-Sequencing

Ikaros chromatin immunoprecipitation (ChIP) was performed as described previously (Harker et al., 2002) with some modifications. The following antibodies were used to study histone modifications: anti-H3K4me3 (Abcam ab8580 or Millipore 07-473), anti-H3K9/K14Ac (Millipore 06-599), anti-H3K27me3 (Millipore 07-449), and anti-H3K36me3 (abcam ab9050). For ChIP-sequencing, chromatin from 2 × 10^7 to 2 × 10^8 cells was used per IP. Precipitated DNA and an equivalent amount of whole genomic DNA were amplified with the DNA Sample Prep Kit (Illumina or New England Biolabs). Amplified samples were run on the Genome Analyzer at Systems Biology Lab, Harvard University. Image analysis and base calling were performed

with the Illumina Pipeline v1.6. Single-end 32 bp alignment with mouse mm9 assembly was conducted with ELAND software. Antibody-enriched regions and signal peaks were identified by MACS algorithm with input as control (Zhang et al., 2008). For data visualization, properly shifted tags were counted along the chromosome, and tag counts in wiggle format were uploaded into Affymetrix IGB.

Expression and Reporter Assays

The following vectors were used for expression and reporter activity studies: (1) pGALuc, a Notch activity reporter plasmid with six tandem RBP-J binding sites driving *Luciferase* expression was kindly provided by A. Ferrando (Columbia University, NY) with permission of T. Honjo (Mizutani et al., 2001). (2) pCS2-E1c (mNotch1-canonical full-length Notch1) and pCS2-E1c 6MT (canonical full-length Notch1 with 6 tandem myc-tag epitopes inserted after amino acid 2183 at the C-terminal part of the protein) were kindly provided by R. Kopan (Kopan et al., 1996). (3) MIG and MIG ICN retroviruses were kindly provided by M. Toribio and W. Pear (Aster et al., 2000). (4) MIG E1c. The E1c cDNA was cloned from the pCS2 vector into the MIG RI vector. (5) MIG E1a, PCS2 E1a and PSC2 E1a 6MT. Notch1 cDNA with the alternative E1a-E3 5′ end was cloned into MIG RI, pCS2 and pCS2 6MT. (6) MIG E25 Notch1. A cDNA representative of the intragenic transcript spanning exon 25 through exon 34 was cloned into the MIG RI retrovirus.

The Notch1 expression plasmids were cotransfected in HEK293 or U2 OS cells, together with the RBP-J Luciferase-reporter pGALuc, and 24 hr later cells were harvested for luciferase and protein analysis.

Primers

All primers used for RT-PCR, 5′ RACE, probe generation, and candidate ChIP are listed in Table S1.

SUPPLEMENTAL INFORMATION

Supplemental Information includes Supplemental Experimental Procedures, seven figures, and one table and can be found with this article online at doi:10.1016/j.immuni.2010.11.008.

ACKNOWLEDGMENTS

This work was supported by NIH-R01-AI1380342 to K.G and by SAF2009-10708 to CNIC and J.M.R and by the European Research Council under the European Community Seventh Framework Programme (FP7/2007-2013)/ERC Grant 208259 to M.V. The CNIC is supported by the Spanish Ministry of Science and Innovation and the Pro-CNIC Foundation. P.G.A. is supported by a Ramón y Cajal Grant and A.F.J. by an NIH training grant in Transplantation Biology. We thank T. Honjo, R. Kopan, A. Ferrando, W. Pear, M.L. Toribio, F. Gounari, and M. Dose for providing reagents used in this study and to B. Czyzewski for mouse husbandry. We also thank B. Morgan, M. Dose, I. Joshi and T. Yoshida for review of the manuscript.

Received: May 21, 2010
Revised: August 12, 2010
Accepted: September 15, 2010
Published online: November 18, 2010

REFERENCES

Amsen, D., Antov, A., and Flavell, R.A. (2009). The different faces of Notch in T-helper-cell differentiation. Nat. Rev. Immunol. *9*, 116–124.

Aster, J.C., Xu, L., Karnell, F.G., Patriub, V., Pui, J.C., and Pear, W.S. (2000). Essential roles for ankyrin repeat and transactivation domains in induction of T-cell leukemia by notch1. Mol. Cell. Biol. *20*, 7505–7515.

Beverly, L.J., and Capobianco, A.J. (2003). Perturbation of Ikaros isoform selection by MLV integration is a cooperative event in Notch(IC)-induced T cell leukemogenesis. Cancer Cell *3*, 551–564.

Bray, S.J. (2006). Notch signalling: A simple pathway becomes complex. Nat. Rev. Mol. Cell Biol. *7*, 678–689.

Campos, E.I., and Reinberg, D. (2009). Histones: Annotating chromatin. Annu. Rev. Genet. *43*, 559–599.

Chari, S., and Winandy, S. (2008). Ikaros regulates Notch target gene expression in developing thymocytes. J. Immunol. *181*, 6265–6274.

Ciofani, M., and Zúñiga-Pflücker, J.C. (2005). Notch promotes survival of pre-T cells at the beta-selection checkpoint by regulating cellular metabolism. Nat. Immunol. *6*, 881–888.

de Boer, J., Williams, A., Skavdis, G., Harker, N., Coles, M., Tolaini, M., Norton, T., Williams, K., Roderick, K., Potocnik, A.J., and Kioussis, D. (2003). Transgenic mice with hematopoietic and lymphoid specific expression of Cre. Eur. J. Immunol. *33*, 314–325.

De Strooper, B., Annaert, W., Cupers, P., Saftig, P., Craessaerts, K., Mumm, J.S., Schroeter, E.H., Schrijvers, V., Wolfe, M.S., Ray, W.J., et al. (1999). A presenilin-1-dependent gamma-secretase-like protease mediates release of Notch intracellular domain. Nature *398*, 518–522.

Dumortier, A., Jeannet, R., Kirstetter, P., Kleinmann, E., Sellars, M., dos Santos, N.R., Thibault, C., Barths, J., Ghysdael, J., Punt, J.A., et al. (2006). Notch activation is an early and critical event during T-Cell leukemogenesis in Ikaros-deficient mice. Mol. Cell. Biol. *26*, 209–220.

Fortini, M.E., and Artavanis-Tsakonas, S. (1994). The suppressor of hairless protein participates in notch receptor signaling. Cell *79*, 273–282.

Garbe, A.I., Krueger, A., Gounari, F., Zúñiga-Pflücker, J.C., and von Boehmer, H. (2006). Differential synergy of Notch and T cell receptor signaling determines alphabeta versus gammadelta lineage fate. J. Exp. Med. *203*, 1579–1590.

Georgopoulos, K. (2009). Acute lymphoblastic leukemia–On the wings of Ikaros. N. Engl. J. Med. *360*, 524–526.

Georgopoulos, K., Bigby, M., Wang, J.H., Molnar, A., Wu, P., Winandy, S., and Sharpe, A. (1994). The Ikaros gene is required for the development of all lymphoid lineages. Cell *79*, 143–156.

Gómez-del Arco, P., Koipally, J., and Georgopoulos, K. (2005). Ikaros SUMOylation: Switching out of repression. Mol. Cell. Biol. *25*, 2688–2697.

Guenther, M.G., Levine, S.S., Boyer, L.A., Jaenisch, R., and Young, R.A. (2007). A chromatin landmark and transcription initiation at most promoters in human cells. Cell *130*, 77–88.

Harker, N., Naito, T., Cortes, M., Hostert, A., Hirschberg, S., Tolaini, M., Roderick, K., Georgopoulos, K., and Kioussis, D. (2002). The CD8alpha gene locus is regulated by the Ikaros family of proteins. Mol. Cell *10*, 1403–1415.

Joshi, A.A., and Struhl, K. (2005). Eaf3 chromodomain interaction with methylated H3-K36 links histone deacetylation to Pol II elongation. Mol. Cell *20*, 971–978.

Kim, J., Sif, S., Jones, B., Jackson, A., Koipally, J., Heller, E., Winandy, S., Viel, A., Sawyer, A., Ikeda, T., et al. (1999). Ikaros DNA-binding proteins direct formation of chromatin remodeling complexes in lymphocytes. Immunity *10*, 345–355.

Kleinmann, E., Geimer Le Lay, A.S., Sellars, M., Kastner, P., and Chan, S. (2008). Ikaros represses the transcriptional response to Notch signaling in T-cell development. Mol. Cell. Biol. *28*, 7465–7475.

Kopan, R., Schroeter, E.H., Weintraub, H., and Nye, J.S. (1996). Signal transduction by activated mNotch: Importance of proteolytic processing and its regulation by the extracellular domain. Proc. Natl. Acad. Sci. USA *93*, 1683–1688.

Laky, K., and Fowlkes, B.J. (2008). Notch signaling in CD4 and CD8 T cell development. Curr. Opin. Immunol. *20*, 197–202.

Lee, P.P., Fitzpatrick, D.R., Beard, C., Jessup, H.K., Lehar, S., Makar, K.W., Pérez-Melgosa, M., Sweetser, M.T., Schlissel, M.S., Nguyen, S., et al. (2001). A critical role for Dnmt1 and DNA methylation in T cell development, function, and survival. Immunity *15*, 763–774.

Malstrom, S., Tili, E., Kappes, D., Ceci, J.D., and Tsichlis, P.N. (2001). Tumor induction by an Lck-MyrAkt transgene is delayed by mechanisms controlling the size of the thymus. Proc. Natl. Acad. Sci. USA *98*, 14967–14972.

Mantha, S., Ward, M., McCafferty, J., Herron, A., Palomero, T., Ferrando, A., Bank, A., and Richardson, C. (2007). Activating Notch1 mutations are an early

event in T-cell malignancy of Ikaros point mutant Plastic/+ mice. Leuk. Res. *31*, 321–327.

Mendenhall, E.M., and Bernstein, B.E. (2008). Chromatin state maps: New technologies, new insights. Curr. Opin. Genet. Dev. *18*, 109–115.

Mizutani, T., Taniguchi, Y., Aoki, T., Hashimoto, N., and Honjo, T. (2001). Conservation of the biochemical mechanisms of signal transduction among mammalian Notch family members. Proc. Natl. Acad. Sci. USA *98*, 9026–9031.

Mullighan, C., and Downing, J. (2008). Ikaros and acute leukemia. Leuk. Lymphoma *49*, 847–849.

Nam, Y., Sliz, P., Song, L., Aster, J.C., and Blacklow, S.C. (2006). Structural basis for cooperativity in recruitment of MAML coactivators to Notch transcription complexes. Cell *124*, 973–983.

Ng, S.Y., Yoshida, T., Zhang, J., and Georgopoulos, K. (2009). Genome-wide lineage-specific transcriptional networks underscore Ikaros-dependent lymphoid priming in hematopoietic stem cells. Immunity *30*, 493–507.

Palomero, T., Lim, W.K., Odom, D.T., Sulis, M.L., Real, P.J., Margolin, A., Barnes, K.C., O'Neil, J., Neuberg, D., Weng, A.P., et al. (2006). NOTCH1 directly regulates c-MYC and activates a feed-forward-loop transcriptional network promoting leukemic cell growth. Proc. Natl. Acad. Sci. USA *103*, 18261–18266.

Radtke, F., Wilson, A., Stark, G., Bauer, M., van Meerwijk, J., MacDonald, H.R., and Aguet, M. (1999). Deficient T cell fate specification in mice with an induced inactivation of Notch1. Immunity *10*, 547–558.

Reschly, E.J., Spaulding, C., Vilimas, T., Graham, W.V., Brumbaugh, R.L., Aifantis, I., Pear, W.S., and Kee, B.L. (2006). Notch1 promotes survival of E2A-deficient T cell lymphomas through pre-T cell receptor-dependent and -independent mechanisms. Blood *107*, 4115–4121.

Robey, E. (1999). Regulation of T cell fate by Notch. Annu. Rev. Immunol. *17*, 283–295.

Sambandam, A., Maillard, I., Zediak, V.P., Xu, L., Gerstein, R.M., Aster, J.C., Pear, W.S., and Bhandoola, A. (2005). Notch signaling controls the generation and differentiation of early T lineage progenitors. Nat. Immunol. *6*, 663–670.

Sandelin, A., Carninci, P., Lenhard, B., Ponjavic, J., Hayashizaki, Y., and Hume, D.A. (2007). Mammalian RNA polymerase II core promoters: Insights from genome-wide studies. Nat. Rev. Genet. *8*, 424–436.

Schones, D.E., and Zhao, K. (2008). Genome-wide approaches to studying chromatin modifications. Nat. Rev. Genet. *9*, 179–191.

Sridharan, R., and Smale, S.T. (2007). Predominant interaction of both Ikaros and Helios with the NuRD complex in immature thymocytes. J. Biol. Chem. *282*, 30227–30238.

Tan, J.B., Visan, I., Yuan, J.S., and Guidos, C.J. (2005). Requirement for Notch1 signals at sequential early stages of intrathymic T cell development. Nat. Immunol. *6*, 671–679.

Tanigaki, K., Han, H., Yamamoto, N., Tashiro, K., Ikegawa, M., Kuroda, K., Suzuki, A., Nakano, T., and Honjo, T. (2002). Notch-RBP-J signaling is involved in cell fate determination of marginal zone B cells. Nat. Immunol. *3*, 443–450.

Tanigaki, K., Tsuji, M., Yamamoto, N., Han, H., Tsukada, J., Inoue, H., Kubo, M., and Honjo, T. (2004). Regulation of alphabeta/gammadelta T cell lineage commitment and peripheral T cell responses by Notch/RBP-J signaling. Immunity *20*, 611–622.

Tsuji, H., Ishii-Ohba, H., Ukai, H., Katsube, T., and Ogiu, T. (2003). Radiation-induced deletions in the 5′ end region of Notch1 lead to the formation of truncated proteins and are involved in the development of mouse thymic lymphomas. Carcinogenesis *24*, 1257–1268.

van Tetering, G., van Diest, P., Verlaan, I., van der Wall, E., Kopan, R., and Vooijs, M. (2009). Metalloprotease ADAM10 is required for Notch1 site 2 cleavage. J. Biol. Chem. *284*, 31018–31027.

von Boehmer, H. (2009). Notch 1 keeps pro-T cells on track. Immunity *30*, 5–7.

Wallberg, A.E., Pedersen, K., Lendahl, U., and Roeder, R.G. (2002). p300 and PCAF act cooperatively to mediate transcriptional activation from chromatin templates by notch intracellular domains in vitro. Mol. Cell. Biol. *22*, 7812–7819.

Wang, J.H., Nichogiannopoulou, A., Wu, L., Sun, L., Sharpe, A.H., Bigby, M., and Georgopoulos, K. (1996). Selective defects in the development of the fetal and adult lymphoid system in mice with an Ikaros null mutation. Immunity *5*, 537–549.

Weng, A.P., Ferrando, A.A., Lee, W., Morris, J.P., 4th, Silverman, L.B., Sanchez-Irizarry, C., Blacklow, S.C., Look, A.T., and Aster, J.C. (2004). Activating mutations of NOTCH1 in human T cell acute lymphoblastic leukemia. Science *306*, 269–271.

Weng, A.P., Millholland, J.M., Yashiro-Ohtani, Y., Arcangeli, M.L., Lau, A., Wai, C., Del Bianco, C., Rodriguez, C.G., Sai, H., Tobias, J., et al. (2006). c-Myc is an important direct target of Notch1 in T-cell acute lymphoblastic leukemia/lymphoma. Genes Dev. *20*, 2096–2109.

Williams, C.J., Naito, T., Arco, P.G., Seavitt, J.R., Cashman, S.M., De Souza, B., Qi, X., Keables, P., Von Andrian, U.H., and Georgopoulos, K. (2004). The chromatin remodeler Mi-2beta is required for CD4 expression and T cell development. Immunity *20*, 719–733.

Wilson, J.J., and Kovall, R.A. (2006). Crystal structure of the CSL-Notch-Mastermind ternary complex bound to DNA. Cell *124*, 985–996.

Winandy, S., Wu, P., and Georgopoulos, K. (1995). A dominant mutation in the Ikaros gene leads to rapid development of leukemia and lymphoma. Cell *83*, 289–299.

Winandy, S., Wu, L., Wang, J.H., and Georgopoulos, K. (1999). Pre-T cell receptor (TCR) and TCR-controlled checkpoints in T cell differentiation are set by Ikaros. J. Exp. Med. *190*, 1039–1048.

Yashiro-Ohtani, Y., He, Y., Ohtani, T., Jones, M.E., Shestova, O., Xu, L., Fang, T.C., Chiang, M.Y., Intlekofer, A.M., Blacklow, S.C., et al. (2009). Pre-TCR signaling inactivates Notch1 transcription by antagonizing E2A. Genes Dev. *23*, 1665–1676.

Yoshida, T., Ng, S.Y., and Georgopoulos, K. (2010). Awakening lineage potential by Ikaros-mediated transcriptional priming. Curr. Opin. Immunol. *22*, 154–160.

Zhang, Y., Liu, T., Meyer, C.A., Eeckhoute, J., Johnson, D.S., Bernstein, B.E., Nusbaum, C., Myers, R.M., Brown, M., Li, W., and Liu, X.S. (2008). Model-based analysis of ChIP-Seq (MACS). Genome Biol. *9*, R137.